

*promoting access to White Rose research papers*



**Universities of Leeds, Sheffield and York**  
**<http://eprints.whiterose.ac.uk/>**

---

This is the author's version of a Proceedings Paper presented at the **6th Space Agency – MOD Workshop on Wide Band Gap Semiconductors and Components, Noordwijk, The Netherlands.**

Grier, A, Cooper, JD, Lever, L, Valavanis, A, Ikonic, Z, Indjin, D, Harrison, P, Edmunds, C, Shao, J, Tang, L, Gardner, G, Zakharov, D, Manfra, MJ and Malis, O *A scattering rate approach to the understanding of absorption line broadening in near-infrared AlGaIn/GaN quantum wells.* In: UNSPECIFIED 6th Space Agency – MOD Workshop on Wide Band Gap Semiconductors and Components, Noordwijk, The Netherlands.

White Rose Research Online URL for this paper:  
<http://eprints.whiterose.ac.uk/id/eprint/75394>

---

# **A scattering rate approach to the understanding of absorption line broadening in near-infrared AlGaIn/GaN quantum wells**

**6th Space Agency – MOD Workshop on Wideband Gap Semiconductors and Components**

**8-9 October 2012**

**ESA-ESTEC, Noordwijk, The Netherlands**

A. Grier<sup>(1)</sup>, J. D. Cooper<sup>(1)</sup>, L. Lever<sup>(1)</sup>, A. Valavanis<sup>(1)</sup>, Z. Ikonić<sup>(1)</sup>, D. Indjin<sup>(1)</sup>,  
P. Harrison<sup>(1)</sup>, C. Edmunds<sup>(2)</sup>, J. Shao<sup>(2)</sup>, L. Tang<sup>(2)</sup>, G. Gardner<sup>(2)</sup>, D. Zakharov<sup>(2)</sup>,  
M. J. Manfra<sup>(2)</sup>, O. Malis<sup>(2)</sup>

<sup>(1)</sup> University of Leeds  
Leeds, LS2 9JT  
United Kingdom  
*Email: el09a2g@leeds.ac.uk*

<sup>(2)</sup> Purdue University  
West Lafayette, IN 47907-2036  
USA  
*Email: omalis@purdue.edu*

## **INTRODUCTION**

There has been much interest in the advancement of III-Nitride growth technology to fabricate AlGaIn/GaN heterostructures for intersubband transitions (ISBTs). The large conduction band offset in these structures (up to 2 eV) allows transition energies in the near- to the far-infrared region, which have applications from telecommunications, such as in all-optical switches [1], to infra-red detectors for sensing and imaging [2]. To date, ISBT electroluminescence has been elusive and absorption measurements remain an important method to verify band structure calculations. The growth quality can be inferred from the absorption spectrum, which will have line broadening with contributions that are both inhomogeneous (large-scale interface roughness, and non-parabolicity) and homogeneous (electron scattering related lifetime broadening). In the present work we calculated the contributions of various homogeneous broadening mechanisms (electron interaction with longitudinal-optical (LO) phonons, acoustic phonons, impurities and alloy disorder) to the full linewidth, and also the contribution of band non-parabolicity, which contributes to the inhomogeneous broadening. Calculations are then compared to the measured absorption spectra of several samples.

## INTERSUBBAND TRANSITIONS

### Absorption calculations and band non-parabolicity

The conduction band offset (CBO) between AlGaIn and GaN allows the formation of one-dimensional quantum wells, in which electronic states are quantised into energy subbands. Intersubband transitions refer to transitions between these states in the conduction band. Intersubband optical absorption has been observed in AlGaIn/GaN [3,4], but to date there has been no demonstration of optical emission. As such, the optimisation of ISBTs in AlGaIn/GaN structures remains an active area of research. The transition linewidth is of particular importance, as it affects the efficiency of passive detector devices, and the peak emission intensity for emitters.

The intersubband absorption between states  $i$  and  $f$  is calculated as in [1]:

$$A_{if}(\omega) = \frac{e^2 \omega}{2\omega \epsilon_0 c} |M_{if}|^2 \int_0^\infty L(\hbar\omega, \hbar\omega_0, k_t^2) F_{if}(k_t^2) dk_t^2 \quad (1)$$

where  $n$  is the refractive index,  $c$  the velocity of light,  $\epsilon_0$  is the vacuum permittivity,  $\hbar\omega$  and  $\hbar\omega_0$  are the energies of the incident photon and the effective intersubband transition, respectively absorption and  $M_{if}$  is the dipole transition matrix element.  $F_{if}$  is the difference of Fermi-Dirac factors for the two states,  $k_t$  is the in-plane wavevector of the electron and  $L$  is the normalized Lorentzian [1]:

$$L(\hbar\omega, \hbar\omega_0, k_t^2) = \frac{\Gamma/2\pi}{(\hbar\omega - \hbar\omega_0)^2 + (\Gamma/2)^2} \quad (2)$$

where  $\Gamma$  is the FWHM broadening of the absorption spectra. The transition energy,  $\hbar\omega_0$ , has an in-plane wavevector,  $k_t$ , dependent component to account for the effects of non-parabolicity in the transverse direction with the form:

$$\hbar\omega_0 = E_{0f} - E_{0i} + \frac{k_t^2 \hbar^2}{2m_{if}} \quad (3)$$

where  $E_{0i}$  and  $E_{0f}$  are the energies of the minima of the initial and final subbands respectively.  $m_{if}^{-1}$  is the difference between the reciprocal in-plane masses in the two subbands,  $m_{if}^{-1} = m_{\parallel f}^{-1} - m_{\parallel i}^{-1}$  with  $m_{\parallel}$  for each subband given by  $m_{\parallel}^*(E) = m^*[1 + (2\alpha' + \beta)(E - U)]$ . For the systems considered in this work,  $\alpha = 0.3 \text{ eV}^{-1}$  and the quantum well material GaN value of  $\beta$  was taken as  $0.049 \text{ eV}^{-1}$  [1]. With non-parabolicity included, the one-dimensional Schrödinger equation becomes a nonlinear eigenvalue problem. An

exact solution was found directly, using a linearization approach [5], and a self-consistent solution to the Poisson equation was found iteratively. Fig. 1. shows that the band non-parabolicity introduces a significant broadening in the absorption spectrum calculated for a typical GaN/AlGaN quantum well at room temperature.

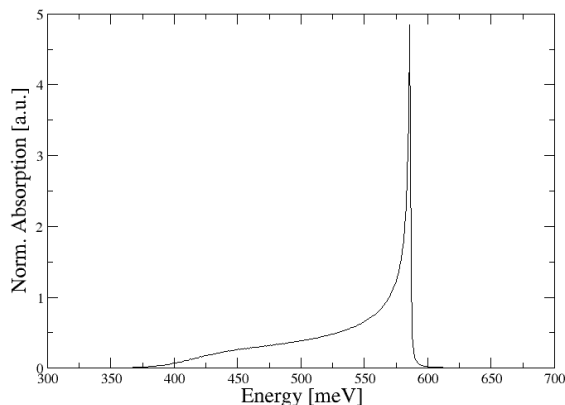


Fig. 1 Typical form of broadening caused by non-parabolicity in intersubband absorption at room temperature for a 2.6-nm GaN well with  $\text{Al}_{0.7}\text{Ga}_{0.3}\text{N}$  barriers and a ground subband sheet charge density of  $3 \times 10^{13} \text{ cm}^{-2}$ .

### Many-body corrections

The large carrier densities that are typical of GaN heterostructures requires that many-body effects be considered for the absorption spectra and the exchange interaction is included as a perturbation to the calculated energy eigenvalues as in [3]. The experimental peak absorption energy will not be the same as the subband splittings due to the depolarization shift,  $\alpha$ , and the excitonic shift  $\beta$ . The effective resonant absorption energy used by the Lorentzian in (2) is given by [3]:

$$\hbar\omega_0 = \hbar\omega_{12}\sqrt{1 + \alpha - \beta} \quad (4)$$

where  $\hbar\omega_{12}$  is the original subband splitting. The depolarisation shift typically introduces a blueshift to the transition due to resonant screening by the electron plasma and the excitonic correction causes a transition redshift due to interaction with the ground quasi-hole and their numerical implementation can be found in [3]. Coulombic scattering mechanisms are also affected by large carrier densities and a screening length is included in their calculation.

## LINewidth BROADENING

Interface roughness will result in a variation of quantum well width in the transverse direction. The broadening from this long-range interface roughness can be modelled by calculating the various transition energies for different well widths (which can be determined from TEM as a first approximation) and calculating the absorption profile with weighted contributions from each width resulting in a Gaussian profile. In addition to this, there is lifetime broadening due to electron scattering between states which is calculated as:

$$\Gamma_{ij} \geq \hbar \left( \frac{1}{\tau_i} + \frac{1}{\tau_j} \right) \quad (5)$$

where  $\tau_i$  is the lifetime of the  $i^{\text{th}}$  state and  $\Gamma$  is the Lorentzian Gamma in (2). These contributions are calculated first and it is then asserted that the remaining linewidth needed to match the experimental results comes from interface roughness.

### Scattering Mechanisms

Scattering is a random change in state which is caused by a perturbation to the normal Hamiltonian of the electron. This perturbation can be caused by electron interaction with LO phonons, acoustic phonons, impurities and alloy disorder effects. The implementation of these for the present work can be found in [6] and we consider contributions to lifetime only from intersubband scattering. Phonons are quanta of vibrational energy which cause periodic variations in strain that introduce scattering by perturbing the conduction band. The peak scattering rate will occur when the energy difference between subbands matches that of the material's phonon energy (90 meV in GaN) although transitions are still possible beyond resonance. Impurity scattering refers to the perturbation of the electron by ionised donor atoms and is maximised when the impurity profile and the electron wavefunction spatially overlap. Scattering from alloy disorder arises since Al and Ga atoms are distributed randomly in the  $\text{Al}_x\text{Ga}_{1-x}\text{N}$  material producing perturbations in the crystal potential. Due to the large doping densities in the samples modeled it is expected that ionised impurity scattering is the dominant contribution to lifetime broadening. We account for the screening of impurity charge by local carriers with an inverse screening length correction to the scattering wavevector. The suitability of the Thomas-Fermi and Debye-Hückel screening lengths [7] is shown by calculating the linewidth contribution using a varying carrier volume density for each.

## NEAR-INFRARED ABSORPTION

Six samples were grown at Purdue via MBE on free standing hydride vapour phase epitaxial (HVPE) substrates with 2.5 nm  $\text{Al}_{0.7}\text{Ga}_{0.3}\text{N}$  barriers and wells that are estimated to be between 6-10 monolayers (ML) wide. The doping locations, measured peak absorption energies and full-width at half-maximum (FWHM) are shown in Table 1. The second and third columns indicate whether there is continuous doping at  $7 \times 10^{19} \text{ cm}^{-3}$  or delta doping at  $2.3 \times 10^{14} \text{ cm}^{-2}$  present in the well (W) or barrier (B) and its location from the beginning of the well.

Table 1 Parameters for MBE grown samples for delta-doping location study

Sample	Continuous Doping	Delta Doping	Energy (meV)	FWHM (meV)	Norm. Int. Abs. ( $\text{cm}^{-1}$ )
D	W,B	W (1.5nm)	654,920	98	15
E-1	W,B	W (0.5 nm)	672	220	17

Reasonable agreement was found between the calculated and experimental peak absorption energies with many-body correction effects applied. It is important to note that due to the energy difference between the ground subband and donor state, the delta doped charge is unionised. In the edge doped sample the donor ionization energy is only  $\sim 30$  meV below the conduction band edge however, the ground subband is still several hundred meV higher than the conduction band edge at this point and therefore this charge is not ionised. The higher potential regions of the triangular quantum wells results in partial ionisation of the heavy doping which overlaps with the wavefunctions and causes impurity scattering. Broadening due to upper state splitting was negligible, with the first excited states calculated to have a nominal range of 6 meV.

The unexpected large linewidth of the well center doped samples was investigated with transmission electron microscopy (TEM) and compared to that of the edge- doped sample (Fig. 2.) This shows that the edge- delta doped sample has minimal well width variation and it can be assumed the 98 meV FWHM measured for this sample arises from lifetime broadening. In contrast, the centre- delta doped sample has a distribution of well widths with differing subband splittings and modeling this accounts for the extra linewidth measured [8]. The contribution to broadening from interface roughness is expected to be negligible due to the long correlation length of interface roughness.

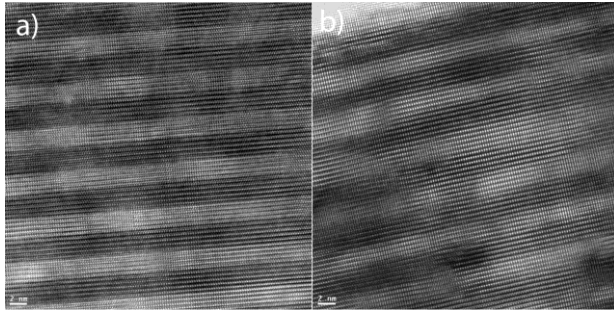


Fig. 2. TEM image of well-edge doped (a) and well-center doped (b) samples

The calculated conduction band profile and the electron wavefunctions are shown in Fig. 3. A single well approach to modelling the subband lifetimes is not valid here since the spatially extended wavefunctions belonging to each well contribute to the number of final states that an electron can scatter into.

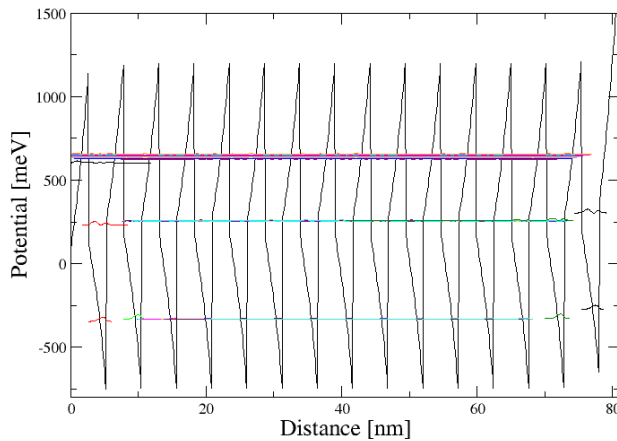


Fig. 3. Calculated conduction band profile of the edge delta doped sample. The 2DEG at the substrate interface was not included here as it does not contribute in the energy region of the linewidth study

The contribution to the lifetimes associated with a transition from a ground subband to a first excited state by impurity scattering is highly dependent on the screening length implemented. Without correcting for the screening of the ionized dopants, the linewidth predicted would be around 8 eV. Fig. 4 shows the relative screening lengths versus carrier volume density for each screening type.

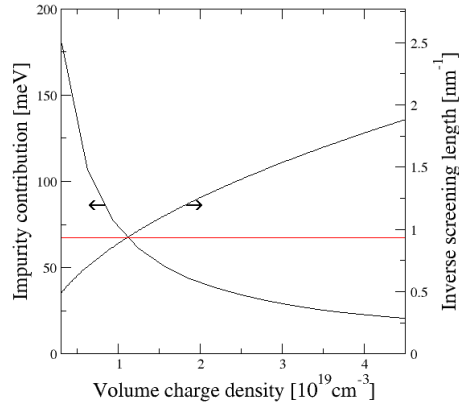


Fig. 4. Impurity contribution and screening length versus volume charge density. Thomas-Fermi screening (red) is independent of the carrier density, unlike Debye screening (black). The charge density for the edge doped device is approximately  $3.5 \times 10^{19} \text{ cm}^{-3}$ .

Thomas-Fermi screening included in the impurity scattering calculation results in a contribution of 67.329 meV to lifetime broadening compared to 15 meV calculated with the Debye screening length. The relative importance of the other scattering mechanisms is shown in Table 2. Given the small scale of the contributions from alloy disorder and phonon scattering, it is clear that only Thomas-Fermi screening is consistent with producing enough broadening in impurity scattering to match experiment. Repeating the method above for the well centre doped structure yields similar results, and this is indirect evidence of the long-range interface roughness shown by TEM in Fig. 2.

Table 2 Homogenous lifetime contributions with Thomas-Fermi screening

Sample	Impurity	CC	ADO	e-LO	ACP	Total
Edge doped	67.329	10.812	0.630	8.171	0.170	87.113
Center doped	69.124	11.240	0.629	8.092	0.146	89.231

## FAR-INFRARED ABSORPTION

Intersubband absorption has also been demonstrated at THz wavelengths of 4.2 and 2.1 THz using  $\text{Al}_{0.1}\text{Ga}_{0.9}\text{N}/\text{Al}_{0.05}\text{Ga}_{0.95}\text{N}/\text{GaN}$  step wells [9] and FWHM of 9 and 3 meV respectively were measured at 4 K. We calculate the lifetime broadening to be from impurity and carrier-carrier scattering (approximately 4.3 and 0.14 meV contributions respectively) for both samples with Debye screening included in the impurity scattering calculation. With the Thomas-Fermi approximation, an impurity contribution of around 8.7 meV is predicted for both samples with minor contributions from other mechanisms.

## SUMMARY

We have used a scattering rate approach to determine the minimum absorption linewidth attainable for intersubband transitions in AlGaN/GaN structures. By comparing with experimental data we have shown that Thomas-Fermi screening of impurity scattering is the right choice for this material at these doping densities and high temperatures. Furthermore, we are able to accurately estimate lifetime broadening in structures operating in the near-infrared through to far-infrared regions which have many possible space applications.

## ACKNOWLEDGEMENTS

The work at Purdue was supported by the NSF awards ECCS-1001431 and DMR-1206919 and from the Defense Advanced Research Project Agency (DARPA) under contract no. D11PC20027.

## REFERENCES

- [1] V. Jovanović, D. Indjin, Z. Ikonić, V. Milanović and J. Radovanović, “Design of GaN/AlGaN quantum wells for maximal intersubband absorption in 1.3-1.55 $\mu\text{m}$  wavelength range,” *Solid State Communications*, vol. 121, pp. 619 – 624, 2002.
- [2] B. S. Williams, “Terahertz quantum-cascade lasers,” *Nature Photonics*, vol. 1 pp. 517-525, 2007.
- [3] M. Tchernycheva *et al.*, “Systematic experimental and theoretical investigation of intersubband absorption in GaN/AlN quantum wells,” *Phys. Rev. B*, vol. 73 pp.125347, March 2006.
- [4] C. Gmachl, H. M. Ng, S. N. G. Chu and A. Y. Cho. “Intersubband absorption at  $\lambda=1.55\ \mu\text{m}$  in well- and modulation-doped GaN/AlGaN multiple quantum wells with superlattice barriers,” *Appl. Phys. Lett.*, vol. 77, pp. 3722 October 2000.
- [5] J. D. Cooper, A. Valavanis, Z. Ikonić, P. Harrison and J. E. Cunningham “Finite difference method for solving the Schrödinger equation with band non-parabolicity in mid-infrared quantum cascade lasers,” *J. Appl. Phys.*, vol. 108, pp. 113109, 2010.
- [6] P. Harrison “Quantum Wells, Wires and Dots,” 2<sup>nd</sup> Ed., John Wiley & Sons Ltd., Chichester 2006.
- [7] J. H. Davies “The physics of low-dimensional semiconductors,” Cambridge University Press, Cambridge 1998.
- [8] M. Cervantes *et al.*, “Effect of doping profile and concentration on the near-Infrared optical properties of AlGaN/GaN Heterostructures,” unpublished.
- [9] H. Machhadani *et al.*, “Terahertz intersubband absorption in GaN/AlGaN step quantum wells,” *Appl. Phys. Lett.*, vol. 97, pp. 191101 November 2010.